ELSEVIER

Journal of Neuroscience Methods 67 (1996) 237–248

JOURNAL OF NEUROSCIENCE METHODS

Spread of stimulating current in the cortical grey matter of rat visual cortex studied on a new in vitro slice preparation

Lionel G. Nowak [1], Jean Bullier [*]

INSERM Unité 371, 'Cerveau et Vision', 18, avenue du Doyen Lépine, 69500 Bron, France

Received 17 January 1996; revised 18 April 1996; accepted 19 April 1996

Abstract

Extracellular electrical stimulation of the cortical grey matter is very often used in electrophysiological studies, but the parameters of the stimulation itself have received only little attention. This study addresses the issue of the spread of stimulating current in rat visual areas 17 and 18a maintained in vitro. The preparation of the slices relied on a protocol making use of several of the means known to limit the effects of ischaemia: Halothane anaesthesia was used during the surgery and intracardiac perfusion was employed to reduce the brain temperature, to increase the intracerebral concentration of glucose and magnesium and to decrease that of calcium. The spread of stimulating current has been determined from strength-distance relationships established for the activation of axons. The strength-distance curves could be fitted by a quadratic relationship, indicating that the threshold current for the activation of an axon increases as the square of the distance separating it from the tip of the stimulating electrode. The slope of the regression line between threshold intensity and squared distance (k coefficient) is highly variable from one axon to another (range 2100–27 500 $\mu A/mm^2$, median 8850 $\mu A/mm^2$). Part of this variability is related to differences in conduction velocity. The theoretical number of axonal branches and axon initial segments activated by a given current intensity has been extrapolated from these experimental results.

Keywords: Intracortical microstimulation; Strength-distance relationship; Slice technique; Corticocortical connections; Conduction velocity

1. Introduction

Electrical stimulation is commonly used in the study of brain physiology for a number of different purposes, such as the study of synaptic potentials and their modifications in the phenomenon of long term potentiation or long-term depression, the identification of the neuronal targets of a given structure, the mapping of motor cortical areas, or to induce or modify a behaviour. Electrical stimulation may also provide a tool in the prosthesis for the blind (Brindley, 1973; Dobelle and Mladejovsky, 1974; Bak et al., 1990).

In the different applications of electrical stimulation, one parameter that must be known is the distance at which a current of a given intensity activates neuronal elements. This effective spread, in turn, determines the number of such elements activated by the stimulation. Knowledge of the spread of stimulating current can be obtained by establishing strength-distance relationships, which consists of measuring the threshold for a given neuronal response as a function of the depth of the stimulating electrode in the structure in which the activated neuronal elements are located. As far as neocortex is concerned, such relationships are known only for the motor cortex (Stoney et al., 1968; Asanuma et al., 1976), but not for any sensory cortex of any mammalian species. The morphological characteristics of neurones and axons differ in motor and sensory cortex. As a consequence, the strength-distance relationship derived for the motor cortex may not apply to sensory cortex. Since a large number of studies are performed in sensory cortex, it appeared important to determine the spread of the effective stimulating current in this structure. For that purpose, we determined strength-distance relationships for the axons of antidromically activated neurones in slices of rat visual cortex. The slice preparation protocol that was used was aimed at reducing the effects of ischaemia that cannot be avoided during this kind of preparation.

[*] Corresponding author. Tel.: (33) 78 13 15 83; Fax: (33) 78 13 15 99.

[1] Present address: Section of Neurobiology, Yale University School of Medicine, C303 Sterling Hall of Medicine, 333 Cedar Street, New Haven, CT 06510, USA. E-mail: Nowak@biomed.med.yale.edu

0165-0270/96/$15.00 Published by Elsevier Science B.V.
PII S0165-0270(96)00065-9

2. Materials and methods

2.1. Brain slice preparation

Male or female, Wistar or Sprague Dawley rats (150–300 g) were anaesthetised with halothane (5% for induction, 2.5–3% during surgery). The aorta was cannulated, usually in less than 30 s, to perfuse the animal with a modified artificial cerebro-spinal fluid (mACSF) from which calcium has been removed, and which has been enriched in glucose and magnesium (flow rate 10 ml/min). Its composition was (in mM): NaCl, 91.7; $NaHCO_3$, 24; NaH_2PO_4, 1.2; KCl, 3; $MgCl_2$, 19; $MgSO_4$, 1; and D-glucose, 25. The rationale for using this solution of perfusion is given in the first part of Section 4. The mACSF was oxygenated for 1 h before the beginning of surgery with a mixture of 95% O_2 and 5% CO_2, and cooled to 3–4°C.

During perfusion, the scalp was removed, the skull was drilled and its upper part removed. During these operations, drops of cold mACSF were applied to accelerate the cooling of the brain. After removal of the skull, the whole brain was carefully removed and glued by its ventral side to a block of agar, itself attached to a vertically oriented support of plastic. 500 μm thick coronal slices were cut with a vibratome (Oxford). The chamber of the vibratome was filled with cooled mACSF that was continuously oxygenated.

Once obtained, the slices were placed in a storage chamber, containing 800 ml of an artificial cerebro-spinal fluid (ACSF) of the following composition (in mM): NaCl, 126; $NaHCO_3$, 24; NaH_2PO_4, 1.2; KCl, 3; $CaCl_2$, 2.5; $MgSO_4$, 1; and D-glucose, 10. This ACSF was continuously bubbled with a 95% O_2-5% CO_2 mixture (pH 7.4). Slices were left in the storage chamber for at least 1 h at room temperature.

For recording, a slice was placed in a submersion-type chamber of 3 ml volume (modified after Llinás and Sugimori, 1980). It rested on a grid in order to be in contact with the ACSF on both sides. The ACSF, similar to that used for storage, was gravity fed at a flow rate of 6–8 ml/min. The temperature was maintained at 33–34°C.

2.2. Recording and stimulation

Micropipettes for intracellular recording were pulled on a BB-CH puller (Mecanex, Geneva) from 1.2 mm OD capillaries with internal microfibre (Clark Electromedical Instruments) and filled with 3 M potassium acetate (DC resistance: 80–120 MΩ). Signals were amplified on an amplifier (Biologic VF 180) followed by a Neurolog device containing amplifiers and filters. The Biologic amplifier contained an active bridge circuit as well as capacity and resistance compensations.

Tungsten-in-glass microelectrodes (Merrill and Ainsworth, 1972) with 15–25 μm exposed tips and plated with platinum black (impedance < 0.5 MΩ at 1000 Hz) were used for extracellular recordings of action potentials. The Neurolog recording system was used for amplification and filtering.

Tungsten-in-glass microelectrodes were also used for electrical stimulation. The glass was removed over a length of 15–25 μm. Electrical stimulation consisted of monopolar, cathodal pulses of 0.2 ms duration. Single pulses were delivered at a frequency of 0.5 or 0.3 Hz through a stimulation isolation unit (Neurolog). Stimulation artefacts were largely reduced by covering the stimulation electrode with conductive paint, except for a few millimeters at the tip, and connecting the paint to the ground (Eide, 1971). For the extracellular recordings, further reduction of the stimulation artefacts was achieved by adjusting the signal filtering.

2.3. Criteria for the identification of antidromic activation

When intracellularly recorded, antidromic action potentials could be unambiguously identified by their constant latency and by the absence of an underlying EPSP. Identification of antidromic action potentials was further facilitated by the presence of the initial segment (IS) spike that sometimes occurred without a soma-dendritic (SD) spike. In some cases, however, IS spikes were not visible, a feature of neurones with high safety factor for transmission of impulses from the initial segment to the somato-dendritic region (Calvin and Sypert, 1976; Lipski, 1981).

The criteria for identifying antidromic action potentials in extracellular recordings were: (a) No variation of latency with current having an intensity equal to 1.5 times the threshold current intensity, the threshold intensity corresponding to the intensity leading to the occurrence of an antidromic action potential in about half the trials. (b) Less than 10% decrease in latency when current intensity was raised from threshold to twice the threshold. (c) A refractory period of less than 3 ms. (d) The ability to sustain a high-frequency (100 Hz or more) stimulation during 200 ms. In a number of well-isolated extracellular recordings, it was also possible to distinguish an inflection in the rising part of the action potential, corresponding to the presence of an IS spike followed by the SD spike (Fig. 1Ad). The validity of these criteria for the identification of antidromic action potentials was confirmed in 5 cases in which recordings were performed in a medium where Ca^{2+} was replaced by 2 mM Mn^{2+}.

The conduction velocity was determined by dividing the distance between stimulating and recording electrode, determined from the cursor of the micromanipulators, by the latency of antidromic activation (measured between the stimulus onset and the foot of the action potential).

3. Results

Strength-distance curves were established for 4 intracellularly and 16 extracellularly recorded neurones. All

were recorded in the supragranular layers of areas 17 or 18a. The 4 neurones that were intracellularly recorded displayed a resting membrane potential between −76 and −80 mV, an input resistance (determined by current injection of −0.1 nA) between 18 and 40 MΩ, and a time constant (determined from current injection of −0.1 nA) between 4.9 and 8 ms. They presented overshooting action potentials, the amplitude of which was between 101 and 122 mV when measured from the resting membrane potential or between 70 and 98 mV when measured from the spike threshold. These neurones displayed properties typical of regular spiking neurones (Connors et al., 1982; McCormick et al., 1985).

The electrical stimulation was always applied in the grey matter. It was used to induce antidromic action potentials in the recorded cells. Strength-distance relationships were determined for 5 neurones involved in the corticocortical connections between area 17 and 18a [a detailed in vitro study of corticocortical connections, including the localisation of the parts of areas 17 and 18a that were in register, will be reported elsewhere (Nowak et al., 1996)]. For these cells, the stimulation was applied in the supragranular layers of one of the two cortical areas while recording was obtained in the other cortical area. For the remaining 15 cells, stimulation and recording were performed in the same area ('intrinsic connections'). For 13 of these cells, the stimulation was applied in the infragranular layers to activate the descending axon. In the remaining 2 cases, the stimulation was applied in the supragranular layers to activate horizontal projection axons.

The separation between stimulating and recording electrodes for the corticocortical cases was between 2.06 and 2.53 mm, and the antidromic spike latencies between 3.66 and 8.6 ms. For the intrinsic connections, the separation between stimulating and recording electrodes was between 0.72 and 1.44 mm (mean ± S.E.M. 1.01 ± 0.09 mm) and the antidromic latency between 1.88 and 5.36 ms (2.64 ± 0.25 ms).

Raw recordings of extracellularly recorded antidromic action potentials are presented in Fig. 1A. These four examples correspond to intrinsic connections. Both successes and failures for antidromic activation obtained with a threshold current intensity are shown superimposed. When the antidromic spike is present, it shows no latency jitter. It can also be seen that, despite the small separation between stimulating and recording electrodes, the stimulation artefact and the action potentials are well separated.

The set up for the experiments used for determining the stimulating current spread is depicted in Fig. 1B. The penetration of the electrode was perpendicular to the slice surface, such that the stimulating electrode remained in the same cortical layer. The stimulating electrode was advanced through the slice in steps of 10 μm. For each of its positions (measured by the depth r), the threshold (I) for inducing an antidromic action potential was determined. The strength-distance curve is the curve relating the threshold intensity I to the depth r of the tip of the stimulating electrode.

An example is shown in Fig. 2. Fig. 2A shows the response of a neurone recorded in the supragranular layers of area 18a to an intracellular depolarising current pulse. Fig. 2B shows the response of the same neurone to an

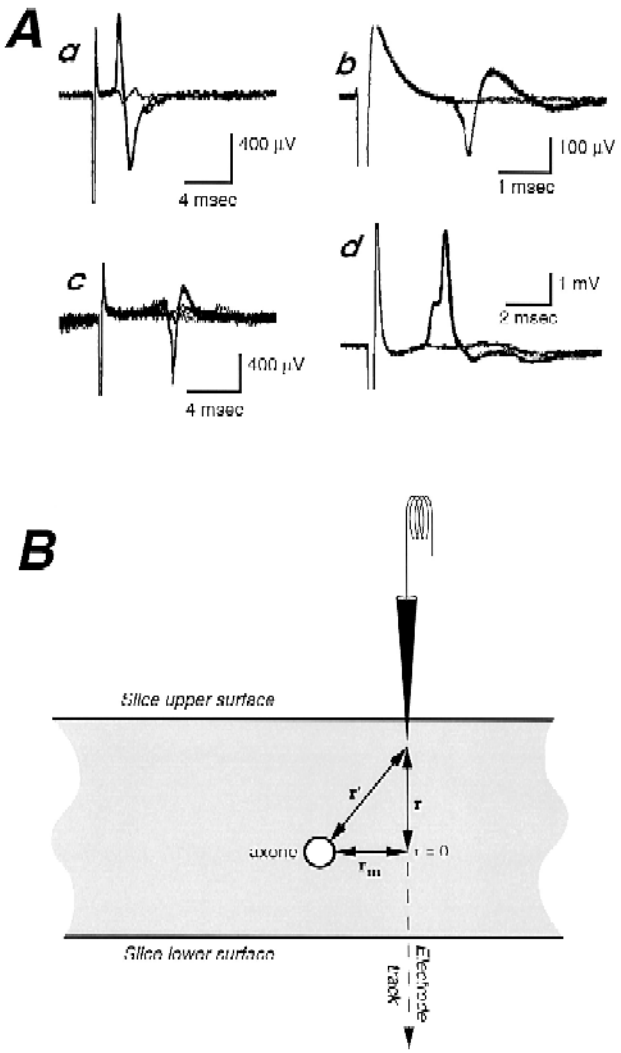

Fig. 1. (A) Raw traces of extracellularly recorded action potentials. The four cases correspond to intrinsic connections, with stimulation applied in the infragranular layer and recordings obtained in the supragranular layer. At least 4 sweeps are shown superimposed. The stimulating intensities correspond to the threshold intensity. Therefore, both successes and failures for antidromic invasion are visible. The action potential of panel Ad corresponds to a case of 'quasi-intracellular' recording. The filters were opened. In these conditions the action potential is positive. The initial segment spike can be distinguished from the somato-dendritic spike by the notch on the rising phase of the action potential. (B) Schematic representation of the set-up used for the determination of stimulating current spread. The section of an axon is represented within a slice (the drawing is not to scale). The stimulating electrode was lowered within the slice along the depth axis r. The threshold for axonal activation, revealed by the presence of an antidromic action potential at the level of the recorded parent neurone, was determined every 10 μm. Further details in text.

electrical stimulation applied in the supragranular layers of area 17. Two sweeps are superimposed. One shows the full antidromic action potential. The other, corresponding to a current intensity slightly lower, shows the initial segment spike in isolation. The slight change in current intensity resulted, in that case, in a slight change of the latency. This case corresponds to the longest corticocortical latency (8.6 ms).

Fig. 2C presents the relationship between the threshold current and the depth of the stimulating electrode tip below the surface of the slice. It shows that, as the stimulating electrode is lowered in the slice, the threshold current required to induce the antidromic action potential decreases from 96 μA at 0.28 mm to a minimum of 15 μA at a depth of 0.35 mm. Then the threshold rises again, up to 89 μA at 0.45 mm.

The shape of the curve shown in Fig. 2C is clearly not linear. This curve has been transformed by normalising the depth with respect to the depth of the minimum threshold and by squaring the normalised depth.

The rationale for this transformation is the following (see also Stoney et al., 1968; Marcus et al., 1979): The activation of an axon by an extracellular stimulation of intensity I results from the extracellular difference in potential induced at a given distance (r' in Fig. 1B) from the tip of the stimulating electrode (e. g., Ranck, 1981). The voltage field is a function of the inverse of the distance r' and is expressed as $V(r') = IR_0/4\pi r'$, R_0 being the specific resistivity of the extracellular medium (in Ω distance units). The corresponding voltage gradient is the relevant parameter for electrical stimulation (Ranck, 1981). The voltage gradient is $\mathrm{d}V/\mathrm{d}r' = -IR_0/4\pi r'^2$. When the stimulating electrode is lowered, the stimulating current I must be modified to be kept at threshold, in such a way that $\mathrm{d}V/\mathrm{d}r'$ remains constant. This constant, A, is equal to $-IR_0/4\pi r'^2$. It follows that

$$I = -A \cdot 4\pi r'^2/R_0 \text{ or } I = kr'^2$$

Thus, the threshold current should be proportional to the square of the distance. k is a coefficient of proportionality (in $\mu A/mm^2$) that characterises the spread of the stimulating current. It relates the threshold current intensity to the distance.

The analysis above assumes that the threshold current is 0 for $r' = 0$. However, the threshold is likely to be different from 0 when the electrode is touching the activated neuronal element. A more proper model is given by $I = kr'^2 + I_0$, with I_0 the threshold current when $r' = 0$.

The distance r' between the stimulating electrode and the axon can be decomposed, such that $r'^2 = r_m^2 + r^2$,

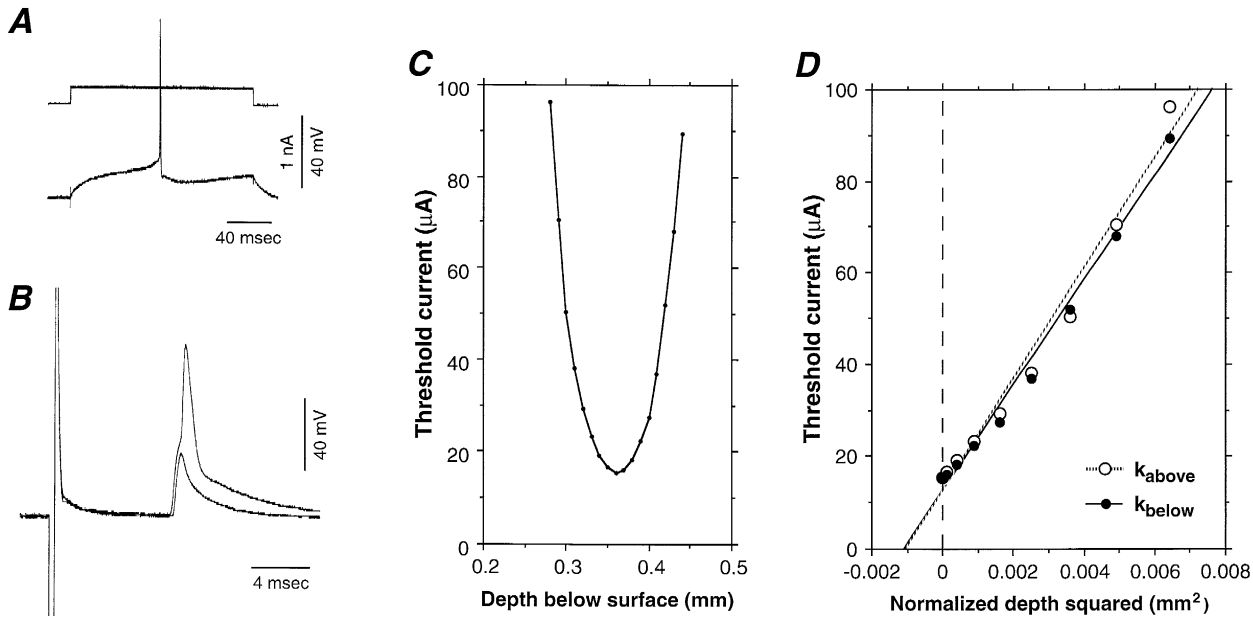

Fig. 2. Example of the determination of the current spread. This cell was intracellularly recorded in the supragranular layer of area 18a. The electrical stimulation was applied in the supragranular layer of area 17. (A) Response of the cell to an intracellular current injection. (B) activation of the cell after extracellular electrical stimulation in area 17. Two sweeps are shown. One shows the initial segment spike in isolation. The other shows the initial segment and the full soma-dendritic spike. (C) Representation of the threshold current for eliciting an antidromic action potential as a function of the depth of the stimulating electrode tip below the surface of the slice. (D) Representation of the threshold current as a function of the squared depth. The depth has been normalised with respect to the lowest threshold depth and squared (0 mm^2 corresponds to 0.35 mm in panel C). Two regression lines are shown. One corresponds to the series of thresholds obtained when the stimulating electrode tip was above the depth where the lowest threshold was observed (k_{above}, 0.28–0.35 mm in panel C), the other to the series of thresholds determined when the electrode tip was below the depth where the lowest threshold was observed (k_{below}, 0.35–0.45 mm on panel C). The relationships between threshold current intensity (I) and the squared depth (r^2) are well fitted by a linear regression. The equations of the regression lines are: $I = 12\,094r^2 + 12.45$ for k_{above} ($r^2 = 0.980$) and $I = 11\,440r^2 + 12.42$ for k_{below} ($r^2 = 0.989$). The slopes correspond to the k coefficient, which characterises the stimulating current spread.

where r is the distance along the electrode track and r_m is the distance between the axis of the electrode track and the axon (Fig. 1B). The threshold current then becomes:

$$I = kr^2 + kr_m^2 + I_0$$

r_m remains constant for a given electrode track. The minimum threshold is obtained when $r = 0$ and corresponds to $kr_m^2 + I_0 = I_m$. The relationship between threshold current and distance can therefore be expressed as

$$I = kr^2 + I_m$$

Fig. 2D shows the relationship between the threshold current and the square of the depth. Two series of dots are shown. The first corresponds to the threshold current measured while the electrode was approaching the depth of the lowest threshold (between 0.28 and 0.35 mm in Fig. 2C). The second corresponds to the threshold current when the electrode was deeper than the minimum threshold depth. The relationship between the square of the normalised depth and the threshold current can be fitted by a line. The slope of this line is k. In this example, k had a value of 12 094 $\mu A/mm^2$ when the electrode was approaching the lowest threshold point (k_{above}), and 11 440 $\mu A/mm^2$ when it was moving away from it (k_{below}). The minimum threshold (I_m) was 12.4 μA.

Another example is illustrated in Fig. 3. The cell was intracellularly recorded in the supragranular layer of area 17 and the electrical stimulation was applied in the infragranular layer of the same area. Fig. 3A shows the response of that cell to an intracellularly injected current pulse. The effect of the extracellular electrical stimulation is shown in Fig. 3B. Two sweeps are shown superimposed. Both were obtained with a threshold current intensity. In one sweep, the stimulation induced an antidromic action potential that rises abruptly from the resting potential with a latency of 2 ms. The initial segment spike is not visible, as already described for the antidromic activation of some neurones (Calvin and Sypert, 1976; Lipski, 1981). In the second sweep, the stimulation failed to induce the action potential. It is possible, then, to see an EPSP, the latency of which is longer by 0.9 ms than the latency of the action potential.

The relationship between the depth of the stimulating electrode and the threshold current is plotted in Fig. 3C. Contrary to the example of Fig. 2, this curve presents 2, possibly 3 minima. This is what could be expected if the stimulating electrode were passing near 3 different branches emanating from the same parent axon (Peterson et al., 1975; Shinoda et al., 1976).

Fig. 3D shows the relationship between the squared depth and the threshold current. The depths have been normalised, such that 0 mm^2 corresponds to 0.15 mm in Fig. 3C. Only one series of dots is shown, which corresponds to the right part of the curve in Fig. 3C (depths between 0.15 and 0.22 mm). There were not enough points between the different minima and maxima of the remain-

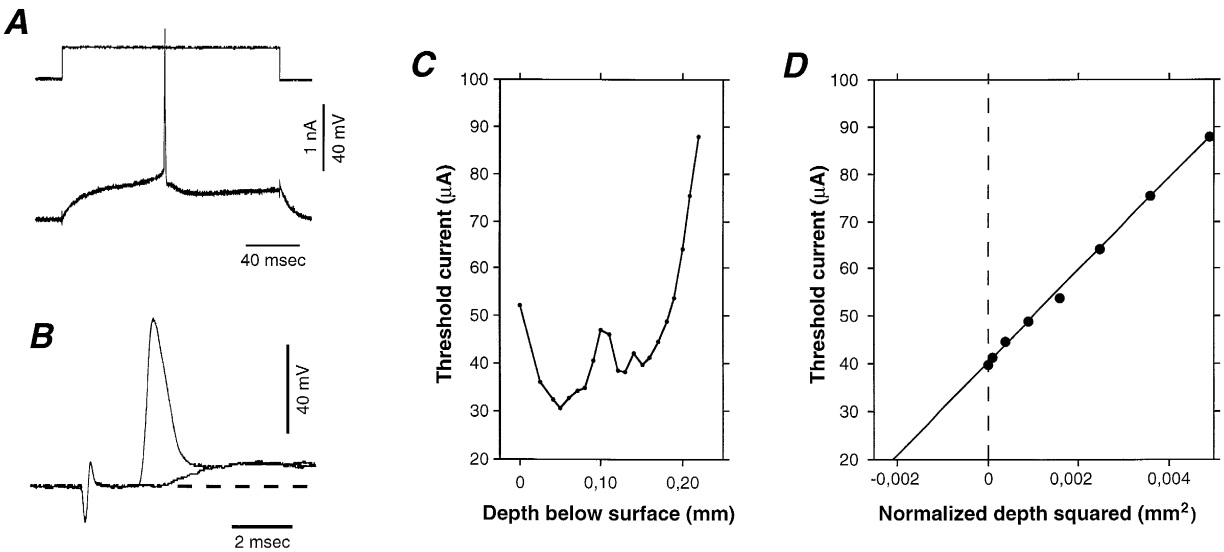

Fig. 3. Another example of the relationship between the distance separating an axon from the stimulating electrode tip and the threshold current to elicit an antidromic action potential. The cell was intracellularly recorded in the supragranular layer of area 17 while the stimulating electrode was located in the infragranular layer of the same area. The response of the cell to an intracellular current injection is presented in A. The antidromic activation of that cell after extracellular electrical stimulation appears in B. Two traces obtained with a threshold current intensity are shown. The action potential is smaller than in A due to deterioration of the recording. However, this deterioration did not prevent the establishment of the strength-distance relationship. (C) Threshold current intensity for antidromic activation presented as a function of the depth of the stimulating electrode tip below the slice surface. (D) Representation of the relationship between threshold current intensity and squared depth. The depth, before being squared, has been normalised with respect to the last minimum encountered (0.15 mm in panel C). The relationship is presented only for the last series of dots (between 0.15 and 0.22 mm) of panel C. The relationship appears linear ($I = 9719r^2 + 39.9$, $r^2 = 0.998$).

ing part of the curve of Fig. 3C for an accurate fitting. Fig. 3D shows that the relationship between the threshold current and the normalised squared distance is linear. The k coefficient in that case was 9719 $\mu A/mm^2$ and the minimum current 39.9 μA.

Summary data about current spread are given in Table 1 and in the histogram of Fig. 4A. For each cell, one (like in Fig. 3) or 2 (as in Fig. 2) values of k could be obtained. The histogram is split to show k values when the electrode was approaching the lowest threshold (k_{above}) and when the electrode was moving away from it (k_{below}). The median value of k_{above} was 6277 $\mu A/mm^2$ ($n = 16$) and the median value of k_{below} was 7952 $\mu A/mm^2$ ($n = 20$). When both measures could be extracted from the same penetration, it was found that the former values were on average lower than the latter (Table 1). This difference proved to be significant (Willcoxon paired test, $p = 0.01$, $n = 15$) and indicates that there is an asymmetry in the strength-distance curves.

As already mentioned, the electrical stimulation was applied either in the same cortical area, or in a cortical area different from the one where the neurone was recorded. The k values obtained for the stimulating depths above the minimum threshold were not significantly different between corticocortical ($n = 5$) and intrinsic ($n = 11$) connections (Mann-Whitney U-test, $p = 0.61$). It was also not different for the stimulating depths below the minimum threshold ($n = 5$ and 15, respectively; $p = 0.83$).

Electrical stimulation was applied either in the supragranular layers or in the infragranular layers. In that case too, there was no significant difference between the k values obtained for the 2 stimulation sites ($p = 0.79$ for k_{above}, $p = 0.50$ for k_{below}; Mann Whitney U-test).

Fig. 4B is a scattergram of the k coefficients computed from the two sides of the quadratic curve, those corresponding to the electrode tip above (k_{above}) vs those corresponding to the electrode tip below (k_{below}) the depth of minimum threshold. There is a significant correlation between k_{above} and k_{below} ($r = 0.805$, $p = 0.0002$ in a t-test on slope coefficient), indicating that the k coefficients obtained above and below the minimum threshold depth are related. However, the slope of the relation is not equal to 1; this confirms the presence of an asymmetry in the strength-distance curves.

The values of the k coefficient appear to be widely scattered (Fig. 4A). To determine whether this is related to some properties of the axons that were stimulated, the relationship between the k coefficient and the axonal conduction velocity of the stimulated axons has been determined and is presented in Fig. 4C. The conduction velocity for corticocortical connections ranged between 0.29 and 0.60 m/s ($n = 4$). The conduction velocity for axons of the intrinsic connections ranged between 0.26 and 0.47 m/s (mean ± S.E.M. 0.37 ± 0.07 m/s, $n = 12$). Similarly to that established by Davies and Kubin (1988), the relationship is presented for the logarithmic values of both

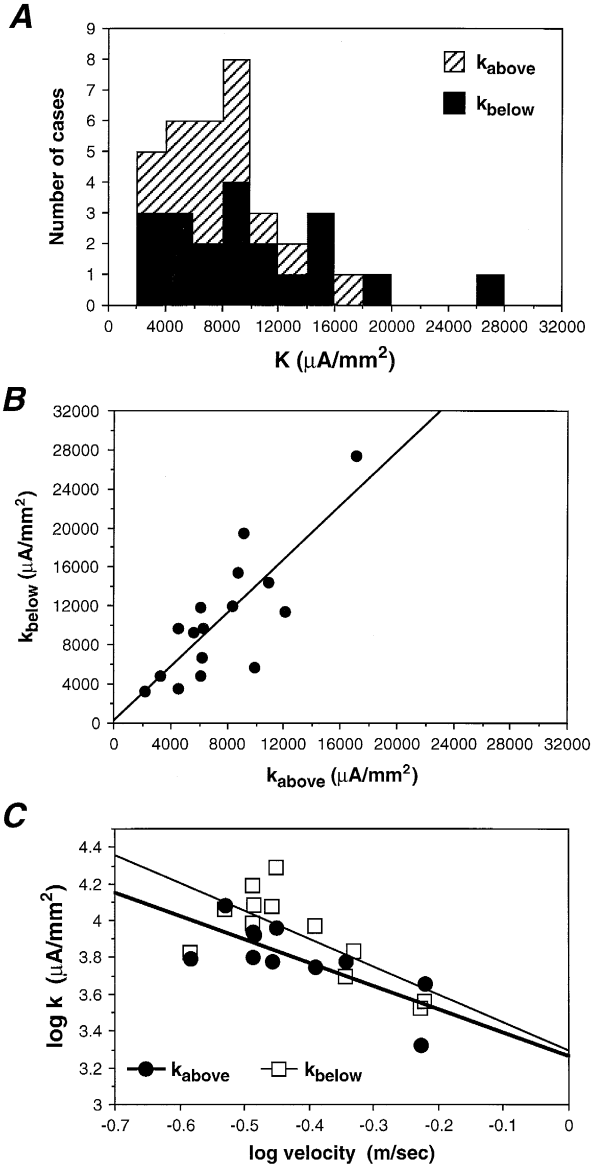

Fig. 4. Summary data on k coefficient. (A) Distribution of k coefficient values. Values of k determined when the different positions of the stimulating electrode tip were above the depth where the lowest threshold was obtained are shown in hatched bars (k_{above}). Those corresponding to positions of the tip of the stimulating electrode below the depth of the lowest threshold are shown in black (k_{below}). (B) Scattergram of the values of k_{below} as a function of the values of k_{above}. The relationship is significant ($k_{below} = 1.376.k_{above} + 267$; $r^2 = 0.648$; $p = 0.0002$). (C) relationship between k coefficient and conduction velocity of the activated axons. The sample size is smaller than in A because electrode separation has not been measured in 4 cases. Since the distributions of k_{above} and k_{below} are significantly different, the relationship has been established for both and is significant in both cases. Best fit equations are: $\log(k) = -1.265 \cdot \log(v) + 3.263$ ($r^2 = 0.569$) for k_{above} and $\log(k) = -1.511 \cdot \log(v) + 3.296$ ($r^2 = 0.526$) for k_{below}.

velocity and k coefficient. Since the k_{above} and k_{below} coefficients are different, a regression line is shown for each. Fig. 4C shows that there is a significant correlation between these two parameters, for both the values of k_{above} ($r = -0.754$, $p = 0.007$) and of k_{below} ($r = -0.725$, $p =$

Table 1
Values of k coefficient ($\mu A/mm^2$) after stimulation of the cortical grey matter

	Number	Mean	S.D.	S.E.M.	Minimum	Maximum	Median
k_{above} and $k_{below,all}$	36	9073	5276	879	2121	27478	8550
$k_{above,all}$	16	7556	3745	936	2121	17065	6277
$k_{below,all}$	20	10289	6058	1354	3359	27478	7952
$k_{above,corticocortical}$	5	8911	5959	2664	2121	17065	8747
$k_{below,corticocortical}$	5	12283	9948	4449	3359	27478	11440
$k_{above,intrinsic}$	11	6935	2345	707	3230	10909	6224
$k_{below,intrinsic}$	15	9625	4431	1144	3560	19473	9705

S.D. standard deviation; S.E.M., standard error to the mean.

0.007). This indicates that the neurones having the fastest conduction velocity are also those displaying the lowest k values. In other words, for a given intensity of stimulating current, the fast conducting axons are activated farther away from the tip of the stimulating electrode than axons displaying a slow conduction velocity.

4. Discussion

4.1. Technical comments about the slice preparation

The main requirement of the method we used for the preparation of brain slices was to prevent, as much as possible, the effects of ischaemia and to allow a precise and gentle dissection of the brain that is necessarily time consuming. This requires some comments, first on the effects of ischaemia and second on how it is possible to delay these effects.

Numerous studies have shown how ischaemia can lead to neuronal death (for review, see Hansen, 1985; Hochachka, 1986; Rothman and Olney, 1986, Rothman and Olney, 1987; Choi, 1988, Choi, 1990; Meyer, 1989; Siesjö and Bengtsson, 1989; Siesjö et al., 1989; McDonald and Johnston, 1990; Schmidt-Kastner and Freund, 1991; Hammond et al., 1994; Martin et al., 1994; Szatkowski and Attwell, 1994). The sequence of events leading to ischaemic cell death starts with the depletion of the energy-rich compounds. It leads, after a short delay, to a compromised regulation of ionic concentrations. One consequence of this is the reversion of the transport system of excitatory amino acids, the concentration of which dramatically increases during oxygen and/or glucose suppression. The involvement of the excitatory amino acids and of the glutamate receptors, particularly of the NMDA receptor, in the pathophysiology of ischaemia is now well documented. The activation of glutamate receptors leads to a massive entry of sodium inside the cells, which is accompanied by that of chloride and water. This produces a neuronal swelling that can, by itself, lead to neuronal death although it can also be reversed. However, neuronal death appears to be mainly the consequence, during and after ischaemia, of calcium entry through NMDA receptors. The resulting excessive intracellular calcium concentration triggers diverse and uncontrolled enzymatic processes leading, among others, to the over-production of free radicals.

The deleterious consequences of ischaemia can be delayed by different ways. The first one is the use of anaesthetics like the halothane we used (Freund et al., 1990). A second one consists of increasing the concentration of magnesium and reducing that of calcium (Kaas and Lipton, 1982; Rothman, 1983; Vacanti and Ames, 1984; Tsuda et al., 1991). High magnesium concentrations are also protective against excitotoxic effects of NMDA in vivo (Wolf et al., 1990). High magnesium concentration should be effective by antagonising voltage-sensitive calcium channels and by reducing ion influx through the NMDA receptor (Nowak et al., 1984; McNamara and Dingledine, 1990). Reduction of the extracellular calcium concentration should also reduce synaptic transmission (Richards and Sercombe, 1970; Dingledine and Somjen, 1981) and reduce its intracellular concentration. The third way is the use of hypothermia, which proves to protect efficiently against ischaemia as reported in a number of studies (Bering, 1974; Siebke et al., 1975; Young et al., 1983; Vacanti and Ames, 1984; Busto et al., 1987). Hypothermia is protective first by reducing the metabolic activity (Klatzo et al., 1968; Bering, 1974; Hägerdal et al., 1975a,b), such that the duration during which energy-rich compounds remains available increases (Michenfelder and Theye, 1970; Carlson et al., 1976; Berntman et al., 1981), and second by decreasing neuronal activity and synaptic transmission (Benita and Condé, 1972; Gähwiler et al., 1972; Fujii, 1977; Girard and Bullier, 1989). Hypothermia has also been shown to reduce the amount of glutamate released during ischaemia (Busto et al., 1989). The fourth way to counteract the effects of ischaemia, at least in vitro, consists of increasing the glucose concentration (Schurr et al., 1987).

There are two periods of ischaemia in our protocol. The first one corresponds to the delay between the opening of the heart and the beginning of the perfusion through the aorta. It lasts less than 30 s and should be of no consequence. Once perfusion has begun, oxygen and glucose are delivered to the brain. This allows, in contrast to what occurs in other protocols, a gentle and precise dissection of the skull and dura matter. The second period of ischaemia lasts from 5 min to up to 30 min. It corresponds to the period during which slices are cut once the brain has been removed from the skull. However, the brain should be protected against this second period of ischaemia since the perfusion has cooled it, loaded it with glucose and magnesium, and reduced the calcium concentration. Using this protocol, we obtained in more than 90% of the experiments slices that displayed satisfying neuronal activity, as can be determined by extra- and intracellular recordings. Slices that were obtained up to 1 h after the beginning of surgery gave extra- and intracellular recordings having the

same quality as those recorded on slices obtained more rapidly. This indicates that our protocol effectively protected neurones against long-lasting ischaemia.

4.2. Spread of stimulating current

Whether a neuronal element is activated by a given intensity of stimulating current depends on the distance between that element and the stimulating electrode. One way to estimate at what distance a current is effectively activating neuronal elements is to establish strength-distance relationships. The relationships we obtained for rat cortical axons show that the threshold current intensity can be related to the square of the distance separating the stimulating electrode from the element activated ($I = kr^2 + I_m$). That the threshold current varies as a function of the square of the distance has been observed by others (Stoney et al., 1968; Armstrong et al., 1973; Marcus et al., 1979, Hentall et al., 1984). Using the relation $I^2 = kr^2 + I_m$, as suggested by Bean (1974), gave less satisfactory results.

In a number of cases, like in Fig. 2, the fitting of the strength-distance curve with a quadratic relationship does not appear perfectly linear. This could be improved by using a power function higher than 2. However, there is no theoretical background to justify a fitting with a power 4 or a power 6 function, whereas a power 2 function is the logical counterpart of the voltage gradient equation that account for the current spread. Nevertheless, the strength-distance relationship is not only determined by the voltage gradient, but also by the membrane properties of the axon, especially its length constant. An equation that takes the axonal properties into account can be found in Hentall (1987). It shows that the threshold current intensity can be linearly proportional to the distance for small separations between the electrode and the axon, while it can be proportional to r^3 for large separations. Therefore, the quadratic relationship would be valid only for intermediate distances. However, the fitting with the quadratic equation we used gave high correlation coefficients: The average was 0.990 ± 0.002 (S.E.M.) for k_{above} (range: 0.966–0.997) and 0.995 ± 0.001 for k_{below} (range: 0.976–0.999). In our sample, 80% of both correlation coefficients were larger than 0.985. Hence, although a simplification, the quadratic equation gave a good approximation of the strength-distance relationship.

The strength-distance curves usually displayed an asymmetry, such that the value of k was on average 1.36 time larger when the electrode was below the depth of lowest threshold (median = 7952 $\mu A/mm^2$) compared with its value when it was above it (median = 6277 $\mu A/mm^2$); in other words, for a given distance, an axon could be activated with less current when the stimulating electrode tip was above it than when it was below. The slices were bathed on both sides by ACSF, and, when one cell was tested, the electrode track was made within the same cortical layer. This does not explain the presence of an excitability gradient parallel to the electrode since the stimulation was applied in a homogeneous medium. One possible explanation for this asymmetry is that the stimulating electrode itself introduced a low resistance pathway, presumably through a film of ACSF between the electrode and the neuronal tissue. In that situation, part of the current would have been shunted and would not have spread homogeneously, such that more current would have been needed to activate the axon. Another explanation for the asymmetry in excitability gradient could be the physical presence of the electrode: As the tip passed the axon, the electrode shaft increased in diameter and distorted the tissue, moving the axon further away from the stimulating tip. The presence of the electrode shaft may also lead to different fields above and below the electrode tip. If these different explanations account for the asymmetry, it is worth mentioning that it is likely to occur in vivo as well as in vitro.

To our knowledge, strength-distance curves have not been established for rat neocortex, and the strength-distance relationship for mammalian visual cortex remained unknown. Strength-distance relationships in cortex have been established for pyramidal tract cells of the cat motor cortex. The k coefficient values obtained for these cells are lower than those we report here: the mean value obtained by Stoney et al. (1968) was 1292 $\mu A/mm^2$ for the direct activation of neurones (most likely at the level of their initial segment; Nowak and Bullier, 1996). Strength-distance curves have also been published for the axon collaterals of pyramidal tract cells in Asanuma et al. (1976) but the values of k were not determined.

Values of k coefficient have been determined for a number of subcortical structures: Axons of spinal cord interneurones were found to have k coefficient as small as 80 $\mu A/mm^2$ (Jankowska and Roberts, 1972). Armstrong et al. (1973) found k values for cerebellar climbing fibres between 190 and 1080 $\mu A/mm^2$. Antidromic activation of pyramidal tract neurones in the spinal cord grey matter gave k values ranging from 300 to 600 $\mu A/mm^2$ (Marcus et al., 1979). Hentall et al. (1984) obtained a mean value of 859 $\mu A/mm^2$ for medullo-spinal neurones. Yeomans et al. (1986) reported values of 400–3000 $\mu A/mm^2$ for the stimulation of axons producing circling behaviour, while axons of the medial forebrain bundle displayed k values between 1000 and 6400 $\mu A/mm^2$. Davies and Kubin (1988) found k coefficient between 100 and 18 750 $\mu A/mm^2$ for axons of nodose ganglion cells. All these results show a large variation of k values between different structures as well as within a single structure. This points to the fact that estimates of current spread established for a given structure must not be applied blindly to another, and suggests that k coefficients depend on the characteristics of the activated axons.

One of these characteristics may be the conduction velocity. The conduction velocity we obtained was 0.39

m/s on average for the whole sample (Fig. 4C). This corresponds to long latency for spike propagation along intrinsic and corticocortical axons, which are similar to those obtained in other studies of visual cortex (Swadlow and Weyand, 1981; Komatsu et al., 1988; Lohmann and Rörig, 1994). According to the relationship established between axonal diameter and conduction velocity (Rushton, 1951; Waxman and Bennett, 1972), it is probable that the axons we have stimulated were of small diameter, with a number of them being unmyelinated.

We found a significant correlation between conduction velocity and k coefficients, such that fast conducting axons have a lower k coefficient. This indicates that a given intensity of stimulation current will activate fast conducting axons but not slowly conducting axons located at the same distance from the stimulating electrode. A correlation between the conduction velocity and k coefficient has been observed in other studies (Stoney et al., 1968; Hentall et al., 1984; Davies and Kubin, 1988; see also Jankowska and Roberts, 1972). The best fit equation we obtained to account for this correlation (Fig. 4) is similar to, although slightly different from, that of Davies and Kubin (1988) (their Fig. 4). In a modelisation study, Rattay (1987) found that the relationship between the k coefficient and conduction velocity is directly related to the axonal diameter. Hence, the fact that larger k coefficient values were observed for rat visual cortex axons compared to those of cat motor cortex neurones (Stoney et al., 1968) can be related to the much faster conduction velocity of the latter (from 5 to 75 m/s: Phillips, 1956, Koike et al., 1968; Takahashi, 1965, Calvin and Sypert, 1976; Deschênes et al., 1979) compared to that of the former.

4.3. Theoretical current spread

The k coefficients obtained experimentally were used to calculate the theoretical current spread, which is illustrated in Fig. 5. For this calculation, it is assumed that $r_m = 0$, in other words that the electrode is touching the axon when the lowest threshold is obtained. This lowest threshold, corresponding to I_0, was assumed to be 1 μA. This value corresponds to the lowest threshold we obtained in different experiments making use of a minimal stimulation strength paradigm (approx. 80 neurones tested in this study and others to be reported elsewhere). The k values that have been used for Fig. 5 correspond to the minimum ($k = 2100$), to the median ($k = 8550$) and to the maximum ($k = 27\,500$) values obtained experimentally. Fig. 5 shows that a current of 10 μA would activate axons located up to 65 μm from the stimulating electrode. 50% of the axons located at a distance of 32 μm from the stimulating electrode would be activated by this current. All the axons should be activated if they are at a distance of 0–18 μm from the stimulating electrode. Similarly, a current of 100 μA should activate all the axons contained within a sphere of 60 μm radius, and 50% of the axons located at 108 μm from the stimulating electrode. These estimations do not take the anodal surround effect into account (Ranck, 1975).

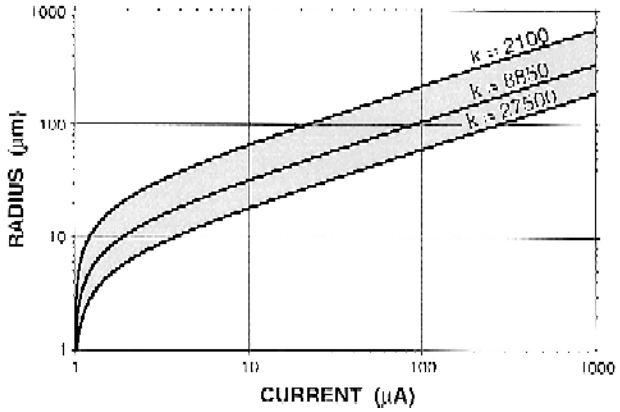

Fig. 5. Theoretical current spread for different values of k. The lines correspond to the equation: radius $= [(I - I_m)/k]^{1/2}$. I_m was set to 1 μA. The calculations are illustrated for 3 different values of k: The minimum (2100 μA/mm^2), the median (8850 μA/mm^2) and the maximum (27 500 μA/mm^2). This figure can be used to estimate the distance at which a given current intensity will activate axons. The minimum radius corresponds to the lowest line ($k = 27\,500$). The light grey area indicates the range of distance at which a decreasing number of axons would be activated. The distance at with one-half of the axons would be activated corresponds to the line for $k = 8850$. Note that these estimations are specific to rat visual cortex.

4.4. Number of neuronal elements activated

Knowing the k coefficient, it is possible to estimate the number of axons and initial segments that are activated by a given current intensity [2]. What must be known is the number of initial segments (i.e. the number of cell bodies) and the number of axons that are contained within the volume in which the electrical stimulation is effective. The number (N) of elements contained within a sphere of radius r is:

$$n = d \cdot (4/3) \cdot \pi \cdot r^3$$

where d is the density (mm^{-3}). $I - I_m = kr^2$ can be transformed into $r = [(I - I_m)/k]^{1/2}$. We then obtain:

$$n = d \cdot (4\pi/3) \cdot \left[(I - I_m)/k\right]^{3/2}.$$

The density of cell bodies and axons in rodent visual cortex appears to be of the order of 10^5 (mouse: Schüz and Palm, 1989; rat: Peters, 1987; Beaulieu, 1993. Note that there is some variability between estimates reported in different studies). The density of axons has not been determined for rat visual cortex (to our knowledge), but

[2] When juxta-somal extracellular electrical stimulation is used, the axon initial segment, rather than the cell body, is likely to be the neuronal element activated (Porter, 1963; Gustafsson and Jankowska, 1976; Swadlow, 1992; Nowak and Bullier, 1996).

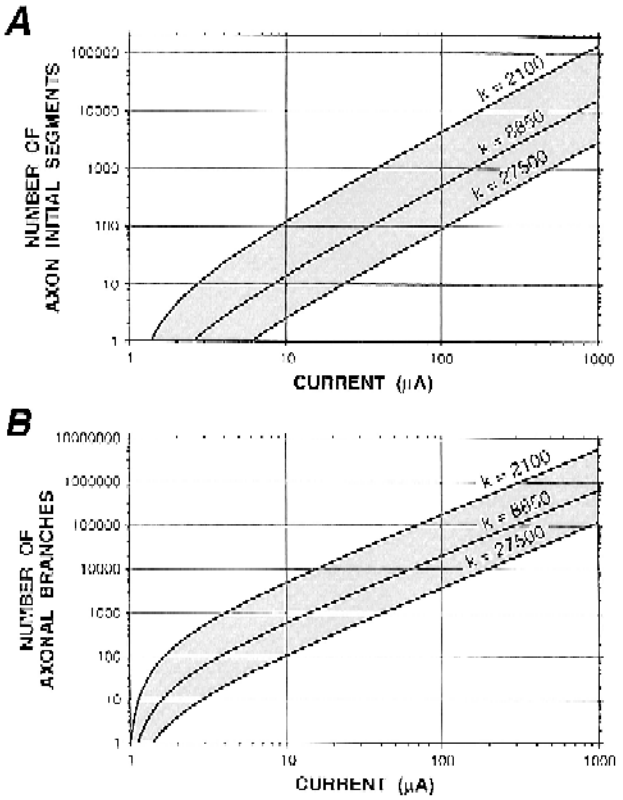

Fig. 6. Theoretical relationship between stimulating current intensity and the number of axon initial segments and axonal branches activated. Calculation according to the equation $N = d \cdot (4p/3) \cdot [(I - I_m)/k]^{3/2}$. Calculation has been performed for 3 values of k determined experimentally: the minimum (2100 $\mu A/mm^2$), the median (8850 $\mu A/mm^2$) and the maximum (27500 $\mu A/mm^2$). I_m was set to 1 μA. Calculation for the number of axon initial segments appears in A, that for axonal branches in B. The light grey area indicates the range of the number of axons activated, which varies depending on the k coefficient characterising these axons. The median number of axons activated given the median k coefficient obtained is this study is indicated by the line for $k = 8850$. The minimum and maximum number of axons activated corresponds to the line for $k = 27500$ and 2100, respectively. The anodal surround effect is not taken into account. Further details in text.

data from mouse visual cortex should yield a correct approximation: Braitenberg and Schüz (1991) reported that there is 4 km of axon/mm^3; if these are randomly distributed in a sphere of 1 mm^3, then the corresponding density is $41.10^5/mm^3$.

The number of axon initial segments that would be activated by a given current intensity is shown in Fig. 6A and that of axons in Fig. 6B. As in Fig. 5, the calculations are shown for 3 values of k: The minimum, the median and the maximum value we obtained experimentally. The value of I_m has been set to 1 μA. From these plots, it can be extrapolated that the number of axon initial segments that would be activated with a current of 10 μA would range from 2–3 ($k = 27500$) to 117 ($k = 2100$), while the median value of k obtained in this study (8850) indicates that a current of 10 μA would activate on average 14 initial segments. Similarly, with a current intensity of 100 μA, the number of initial segments activated would range between 90 and 4280 with a median value of 495. The number of axonal branches (Fig. 6B) activated by a stimulation of 10 μA would range between 100 ($k = 27500$) and 4800 ($k = 2100$) with a median of 560. Finally, a current intensity of 100 μA would activate between 3700 and 176000 axonal branches with a median of 20320.

Acknowledgements

We thank Pascale Giroud and Naura Chounlamountri for help during the experiments, Pierre-Marie Chorrier for help with the mechanic, Christian Urquizar for help with the electronic. This work was supported by H.F.S.P. no. RG 55/94. L.G.N. was supported by a fellowship from the Ministère de la Recherche et de la Technologie and by a fellowship from Fyssen Foundation.

References

Armstrong, D.M., Harvey, R.J and Schild, R.F. (1973) The spatial organisation of climbing fibre branching in the cat cerebellum, Exp. Brain Res., 18: 40–58.

Asanuma, H., Arnold, A. and Zarzecki, P. (1976) Further study on excitation of pyramidal tract cells by intracortical microstimulation, Exp. Brain Res., 26: 443–461.

Bak, M., Girvin, J.P., Hambrecht, F.T., Kufka, C.V., Loeb, G.E. and Schmidt, E.M. (1990) Visual sensation produced by intracortical microstimulation of the human occipital cortex, Med. Biol. Eng. Comput., 28: 257–259.

Bean, C.P. (1974) A theory of microstimulation of myelinated fibres. Appendix in: Azbug, C., Maeda, M., Peterson, B.W. and Wilson, V.J. (1974) Cervical branching of lumbar vestibulospinal axons, J. Physiol. (Lond.), 243: 499–522.

Beaulieu, C. (1993) Numerical data on neocortical neurons in adult rat, with specific reference to the GABA population, Brain Res., 609: 284–292.

Benita, M. and Condé, H. (1972) Effect of local cooling upon conduction and synaptic transmission, Brain Res., 36: 133–151.

Bering, E.A. (1974) Effect of profound hypothermia and circulatory arrest on cerebral oxygen metabolism and cerebrospinal fluid electrolyte composition, J. Neurosurg., 39: 199–207.

Berntman, L., Welsh, F.A. and Harp, J.R. (1981) Cerebral protective effect of low-grade hypothermia, Anesthesiology, 55: 495–498.

Braitenberg, V. and Schüz, A. (1991) Anatomy of the Cortex, Statistics and Geometry, Springer-Verlag, Berlin.

Brindley, G.S. (1973) Sensory effects of electrical stimulation of the visual and paravisual cortex in man. In H. Autrum, R. Jung, W.R. Loewenstein, D.M. MacKay and H.L. Teuber, (Eds), Handbook of Sensory Physiology, Vol. VII/3, Central Processing of Visual Information, part B, Springer-Verlag, Berlin, pp. 583–594.

Busto, R., Dietrich, D., Globus, M.Y.-T., Valdés, I., Scheinberg, P. and Ginsberg M.D. (1987) Small differences in intraischemic brain temperature critically determine the extent of ischemic neuronal injury, J. Cereb. Blood Flow Metab., 7: 729–738.

Busto, R., Globus, M.Y.-T., Dietrich, D., Martinez, E., Valdès, I. and Ginsberg, M.D. (1989) Effect of mild hypothermia on ischemia-induced release of neurotransmitters and free fatty acids in rat brain, Stroke, 20: 904–910.

Calvin, W.H. and Sypert, G.W. (1976) Fast and slow pyramidal tract

neurons: an intracellular analysis of their contrasting repetitive firing properties in the cat, J. Neurophysiol., 39: 420–434.
Carlson, C., Hägerdal, M. and Siesjö, B.K. (1976) Protective effect of hypothermia in cerebral oxygen deficiency caused by arterial hypoxia, Anesthesiology, 44: 27–35.
Choi, D.W. (1988) Calcium mediated neurotoxicity: Relationship to specific channel types and role in ischemic damage, Trends Neurosci., 11: 465–469.
Choi, D.W. (1990) Cerebral hypoxia: Some new approaches and unanswered questions, J. Neurosci., 10: 2493–2501.
Connors, B.W., Gutnick, M.J. and Prince, D.A. (1982) Electrophysiological properties of neocortical neurons in vitro, J. Neurophysiol., 48: 1302–1320.
Davies, R.O. and Kubin, L. (1988) Projection of pulmonary rapidly adapting receptors to the medulla of the cat: an antidromic mapping study, J. Physiol. (Lond.), 373: 63–86.
Deschênes, M., Labelle, A. and Landry, P. (1979) Morphological characterization of slow and fast pyramidal tract cells in the cat, Brain Res., 178: 251–274.
Dingledine, R. and Somjen, G. (1981) Calcium dependence of synaptic transmission in the hippocampal slice, Brain Res., 207: 218–222.
Dobelle, W.H. and Mladejovsky, M.G. (1974) Artificial vision for the blind: electrical stimulation of visual cortex offers hope for a functional prosthesis, Science, 183: 440–444.
Eide, E. (1971) Stimulation and recording with closely spaced microelectrodes, Acta Physiol. Scand., 82: 4A–5A.
Freund, T.F., Buzsaki, G., Leon, A. and Somogyi, P. (1990) Hippocampal cell death following ischemia: Effects of brain temperature and anaesthesia, Exp. Neurol., 108: 251–260.
Fujii, T. (1977) Effects of cooling on guinea pig olfactory cortex maintained in vitro, Electroenceph. Clin. Neurophysiol., 43: 238–247.
Gähwiler, B.H., Mamoon, A.M., Schlapfer, W.T. and Tobias, C.A. (1972) Effect of temperature on spontaneous bioelectric activity of cultured nerve cells, Brain Res., 40: 527–533.
Girard, P. and Bullier, J. (1989) Visual activity in area V2 during reversible inactivation of area 17 in the macaque monkey, J. Neurophysiol., 62: 1287–1302.
Gustafsson, B. and Jankowska, E. (1976) Direct and indirect activation of nerve cells by electrical pulses applied extracellularly, J. Physiol. (Lond.), 258: 33–61.
Hägerdal, H., Harp, J., Nilson, L. and Siesjö, B.K. (1975a) The effect of induced hypothermia upon oxygen consumption in the rat brain, J. Neurochem., 24: 311–316.
Hägerdal, H., Harp, J. and Siesjö, B.K. (1975b) Effect of hypothermia upon organic phosphate, glycolitic metabolites, citric acid cycle intermediates and associated amino acids in rat cerebral cortex, J. Neurochem., 24: 743–748.
Hammond, C., Crépel, V., Gozlan, H. and Ben-Ari, Y. (1994) Anoxic LTP sheds light on the multiple facets of NMDA receptors, Trends Neurosci., 11: 497–503.
Hansen, A.K. (1985) Effect of anoxia on ion distribution in the brain, Physiol. Rev., 65: 101–148.
Hentall, I.D., Zorman, G., Kansky, S. and Field, H.L. (1984) Relations among threshold, spike height, electrode distance, and conduction velocity in electrical stimulation of certain medullospinal neurons, J. Neurophysiol., 51: 968–977.
Hentall, I.D. (1987) Practical modelling of monopolar axonal stimulation, J. Neurosci. Methods, 22: 65–72.
Hochachka, P.W. (1986) Defence strategies against hypoxia and hypothermia, Science, 231: 234–241.
Jankowska, E. and Roberts, W.J. (1972) An electrophysiological demonstration of the axonal projections of single spinal interneurones in the cat, J. Physiol. (Lond.), 222: 597–622.
Kaas, I.S. and Lipton, P. (1982) Mechanisms involved in irreversible anoxic damage to the in vitro rat hippocampal slice, J. Physiol. (Lond.), 332: 459–472.
Klatzo, I., Li, C.-H., Long, D.M., Bak, A.F., Mossakowski, M.J., Parker, L.O. and Rasmussen, L.E. (1968) The effect of hypothermia on electric impedance and penetration of substances from the CSF into the periventricular brain tissue. In A. Lajtha and D.H. Ford (Eds), Progress in Brain Research, Vol. 29, Elsevier, Amsterdam, pp. 385–399.
Koike, H., Okada, Y., Oshima, T. and Takahashi, K. (1968) Accommodative behavior of cat pyramidal tract cells investigated with intracellular injection of currents, Exp. Brain Res., 5: 173–188.
Komatsu, Y., Nakajima, S., Toyama, K. and Fetz, E.E. (1988) Intracortical connectivity revealed by spike-triggered averaging in slice preparations of cat visual cortex, Brain Res., 442: 359–362
Lipski, J. (1981) Antidromic activation of neurones as an analytic tool in the study of the central nervous system, J. Neurosci. Methods, 4: 1–32.
Llinás, R.R. and Sugimori, M. (1980) Electrophysiological properties of in vitro purkinje cell somata in mammalian cerebellar slices, J. Physiol. (Lond.): 305, 171–195.
Lohmann, H. and Rörig, B. (1994) Long-range horizontal connections between supragranular pyramidal cells in the extrastriate visual cortex of the rat, J. Comp. Neurol., 344: 543–558.
Marcus, S., Zarzecki, P. and Asanuma, H. (1979) An estimate of effective spread of stimulating currents. Appendix in: Shinoda, Y., Zarzecki, P. and Asanuma, H. (1979) Spinal branching of pyramidal tract neurons in the monkey, Exp. Brain Res., 34: 59–72.
Martin, R.L., Lloyd, H.G.E. and Cowan, A.I. (1994) The early events of oxygen and glucose deprivation: setting the scene for neuronal death? Trends Neurosci., 17: 251–257.
McCormick, D.A., Connors, B.W., Lighthall, J.W. and Prince, D.A. (1985) Comparative electrophysiology of pyramidal and sparsely spiny stellate neurons of the neocortex, J. Neurophysiol., 54: 782–806.
McDonald, J.W. and Johnston, M.V. (1990) Physiological and pathological roles of excitatory amino acids during central nervous system development, Brain Res. Rev., 15: 41–70.
McNamara, D. and Dingledine, R. (1990) Dual effect of glycine on NMDA-induced neurotoxicity in rat cortical culture, J. Neurosci., 10: 3970–3976.
Merrill, E.G. and Ainsworth, A. (1972) Glass-coated platinum-plated tungsten microelectrodes, Med. Biol. Eng., 10: 662–672.
Meyer, F.B. (1989) Calcium, neuronal hyperexcitability and ischemic injury, Brain Res. Rev., 14: 227–243.
Michenfelder, J.D. and Theye, R.A. (1970) The effects of anaesthesia and hypothermia on canine cerebral ATP and lactate during anoxia produced by decapitation, Anesthesiology, 33: 430–439.
Nowak, L., Bregestovski, P., Ascher, P., Herbert, A. and Prochiantz, A. (1984) Magnesium gates glutamate-activated channels in mouse central neurones, Nature, 307: 462–465.
Nowak, L.G., James, A.C. and Bullier, J. (1996) Corticocortical connections between visual areas 17 and 18a of the rat studied in vitro: Spatial and temporal organisation of functional synaptic responses, submitted.
Nowak, L.G. and Bullier, J. (1996) Axons, but not cell bodies, are activated by electrical stimulation in the cortical grey matter: An in vitro study on rat visual cortex, submitted.
Peters, A. (1987) Number of neurons and synapses in primary visual cortex. In E.G. Jouensand and A. Peters (Eds), Cerebral Cortex, Vol. 6: Further Aspects of Cortical Function, Including Hippocampus, Plenum Press, New York, pp. 267–294.
Peterson, B.W., Maunz, R.A., Pitts, N.G. and Mackel, R.G. (1975) Patterns of projection and branching of reticulospinal neurons, Exp. Brain Res., 23: 333–351.
Phillips, C.G. (1956) Intracellular records from Betz cells in the cat, Q. J. Exp. Physiol., 41: 58–69.
Porter, R. (1963) Focal stimulation of hypoglossal neurones in the cat, J. Physiol. (Lond.), 169: 630–640.
Ranck, J.B. (1975) Which elements are excited in electrical stimulation of

mammalian central nervous system: A review, Brain Res., 98: 417–440.

Ranck, J.B. (1981) Extracellular stimulation. In M.M. Patterson and R.P. Kesner (Eds), Electrical Stimulation Research Techniques, Academic Press, New York, pp. 1–36.

Rattay, F. (1987) Ways to approximate current-distance relations for electrically stimulated fibers, J. Theor. Biol., 125: 339–349.

Richards, C.D. and Sercombe, R. (1970) Calcium, magnesium and the electrical activity of guinea-pig olfactory cortex in vitro, J. Physiol. (Lond.), 211: 571–584.

Rothman, S.M. (1983) Synaptic activity mediates death of hypoxic neurons, Science, 220: 536–537.

Rothman, S.M. and Olney, J.W. (1986) Glutamate and the pathophysiology of hypoxic-ischemic brain damage, Ann. Neurol., 19: 105–111.

Rothman, S.M. and Olney, J.W. (1987) Excitotoxicity and NMDA receptors, Trends Neurosci., 10: 299–302.

Rushton, W.A.H. (1951) A theory of the effects of fibre size in medullated nerve, J. Physiol. (Lond.), 115: 101–122.

Schmidt-Kastner, R. and Freund, T.F. (1991) Selective vulnerability of the hippocampus in brain ischemia, Neuroscience, 40: 599–636.

Schurr, A., West, C.A., Reid, K.H., Tseng, M.T., Reiss, S.J., and Rigor, B.M. (1987) Increased glucose improves recovery of neuronal function after cerebral hypoxia in vitro, Brain Res., 421: 135–139.

Schüz, A. and Palm, G. (1989) Density of neurons and synapses in the cerebral cortex of the mouse, J. Comp. Neurol., 286: 442–455.

Shinoda, Y., Arnold, A.P. and Asanuma, H. (1976) Spinal branching of cortico-spinal axons in the cat, Exp. Brain Res., 26: 215–234.

Siebke, H., Breivik, H., Rod, T. and Lind, B. (1975) Survival after 40 minutes submersion without cerebral sequelae, Lancet, 2: 1275–1277.

Siesjö, B.K. and Bengtsson, F. (1989) Calcium fluxes, calcium antagonists, and calcium related pathology in brain ischemia, hypoglycaemia, and spreading depression: A unifying hypothesis, J. Cereb. Blood Flow Metab., 9: 127–140.

Siesjö, B.K., Agardh, C.-D. and Bengtsson, F. (1989) Free radicals and brain damage, Cerebrovasc. Brain Metab. Rev., 1: 165–211.

Stoney, S.D., Thompson, W.D. and Asanuma, H. (1968) Excitation of pyramidal tract cells by intracortical microstimulation: effective extent of stimulating current, J. Neurophysiol., 31: 659–669.

Swadlow H.A. and Weyand T.H. (1981) Efferent systems of the rabbit visual cortex: Laminar distribution of cells of origin, axonal conduction velocities and identification of axonal branches, J. Comp. Neurol., 203: 799–822

Swadlow, H.A. (1992) Monitoring the excitability of neocortical efferent neurons to direct activation by extracellular current pulses, J. Neurophysiol., 68: 605–619.

Szatkowski, M. and Attwell, D. (1994) Triggering and execution of neuronal death in brain ischemia: two phases of glutamate release by different mechanisms, Trends Neurosci., 17: 359–365.

Takahashi, K. (1965) Slow and fast groups of pyramidal tract cells and their respective membrane properties, J. Neurophysiol., 28: 908–924.

Tsuda, T., Kogure, K., Nishioka, K. and Watanabe, T. (1991) Mg^{2+} administered up to twenty-four hours following reperfusion prevents ischemic damage of the CA1 neurons in the rat hippocampus, Neuroscience, 44: 335–341.

Vacanti, F.X. and Ames, A. (1984) Mild hypothermia and Mg^{++} protect against irreversible damage during CNS ischemia, Stroke, 15: 695–698.

Waxman, S.G. and Bennett, M.V.L. (1972) Relative conduction velocities of small myelinated and non-myelinated fibres in the central nervous system, Nature 238: 217–219.

Wolf, G., Keihoff, G., Fischer, S. and Haas, P. (1990) Subcutaneously applied magnesium protects reliably against quinolinate-induced *N*-methyl-D-aspartate (NMDA)-mediated neurodegeneration and convulsions in rats: are there therapeutical implications? Neurosci. Lett., 117: 207–211.

Yeomans, P., Prior, P. and Bateman, F. (1986) Current-distance relations of axons mediating circling elicited by midbrain stimulation, Brain Res., 372: 95–106.

Young, R.S.K., Olenginski, T.P., Yagel, S.K. and Towfighi, J. (1983) The effect of graded hypothermia on hypoxic-ischemic brain damage: A neuropathology study in neonatal rat, Stroke, 14: 929–934.